UNSTAGGERED CENTRAL SCHEMES FOR ONE-DIMENSIONAL NONLOCAL CONSERVATION LAWS

Said Belkadi [1,§] , **Mohamed Atounti** [2]

[1,2] Mohammed First University-Oujda

Pluridisciplinary Faculty of Nador, MOROCCO

Abstract

We describe a new family of second-order, unstaggered central finite volume methods for one-dimensional nonlocal traffic flow models. The main advantage of the presented method is its ability to evolve the numerical solution on a single grid, avoid solving Riemann problems at the cell interfaces, and alternate between an original and a staggered grid. Our numerical results demonstrate the effectiveness and performance of the suggested method by comparing them favorably to those produced using the original Nessyahu-Tadmor (NT) method.

1. Introduction

Conservation law equations with nonlocal flux are widely investigated because of their utility in simulating physical phenomena such as sedimentation [4], pedestrians [7], and traffic flow [5, 6, 8, 9, 11]. The one-dimensional conservation law equations with nonlocal flux considered in this study are given by:

$$\begin{cases} \partial_t \rho + \partial_x F(\rho, V) = 0, & x \in \mathbb{R},\, t > 0, \\ \rho(0, x) = \rho_0(x), & x \in \mathbb{R}, \end{cases} \tag{1}$$

where

$$V(t,x) = \kappa_\eta * v(\rho)(t,x) = \int_x^{x+\eta} \kappa_\eta(y-x)v(\rho(t,y))dy, \quad \eta > 0,$$

$$F(\rho, V) = f(\rho)V.$$

In (1), t is time, x is the space variables, ρ is the unknown density, and v is the traffic velocity. In addition, we put forward the following assumptions, which ensure the existence and uniqueness of the entropy solution for the Cauchy problem (1), as well as some a priori estimates, namely, L^1, L^∞ as well as total variation estimates obtained in several works (see, e.g.,[1, 5, 6, 8]).

$$g \in C^1(I; \mathbb{R}^+), \quad \text{with} \quad g' \geqslant 0,$$
$$v \in C^2(I; \mathbb{R}^+), \quad \text{with} \quad v' \leqslant 0.$$

In [8], the authors presented an upwind Godunov-type scheme for the numerical resolution of the model (1). The Godunov-type schemes are projecting-evolution methods. Depending on the projection step, we distinguish two Godunov-type schemes: upwind and central schemes. However, most upwind Godunov-type schemes are based on reassembly, which requires solving Riemann problems, a process that is so complicated, time-consuming, and demanding. In contrast, central schemes have an advantage over the corresponding upwind schemes, in which no (approximate) Riemann solvers are required. In prior work [2, 3], we solved model (1) using the Nessyahu-Tadmor (NT) scheme [12], which is a second-order, non-oscillatory central scheme, and the results are in good accord with the results obtained using Godunov's scheme.

However, in NT-type schemes, transitioning from an original grid to a shifted grid is regarded as a flaw. More precisely, if the numerical solution obtained using an NT-type scheme necessitates additional treatment to meet a physical requirement, a synchronization problem arises because any treatment of the updated solution incorporates the solution values computed at various times before [13]. The problem becomes significantly more complex when the original and dual staggered cells are not the same size.

Using both Nessyahu-Tadmor's iteration formulas, the authors of [13] offered an unstaggered application of the NT approach to solving shallow water equations. Touma et al. created a second-order accurate, one-dimensional, unstaggered central scheme for the Euler system with gravity [14]. The approach described in [14] can be seen as a generalization of the process described by Touma et al. [13] and an unstaggered application of the NT scheme.

In this paper, we introduce a new family of central, unstaggered, second-order accurate schemes (UCS) for traffic flow with a non-local flux that prevents NT-type schemes from shifting from an original grid to a shifted grid.

The proposed method is based on the reconstruction method presented in [14], which generates the numerical solution on a single grid. The fundamental idea behind UCS schemes is to grow the numerical solution on a single grid and then use a ghost cell in an intermediate phase before back-projection.

The UCS scheme, like most second-order central schemes for conservation laws, is designed to satisfy the Total Variation Diminishing (TVD) property. The MUSCL (Monotonic Upstream Conservation Laws) reconstruction presented by Van Leer is one technique to accomplish this. This was supplemented by the application of slope limiters, which approximate the spatial derivatives.

This paper is arranged as follows: Section 2 provides a full overview of the suggested method. Section 3 includes numerical tests to test the correctness and stability of this approach. Section 4 contains concluding observations.

2. Second-order central scheme

In this section, we build a new unstaggered central scheme for the nonlocal traffic flow model (1). The proposed method is based on the reconstruction method provided in [13]. We begin by reviewing the NT scheme and then adapting it to the new UCS scheme.

2.1. **Nessyahu-Tadmor scheme.** We divide the computational domain $[a, b]$ into cells of size Δx such that $\eta = N\Delta x$ for some $N \in \mathbb{N}$. $[x_{j-\frac{1}{2}}, x_{j+\frac{1}{2}}]$ represents the jth cell, $x_j = j\Delta x$ the cell centers, $x_{j+\frac{1}{2}} = (j + \frac{1}{2})\Delta x$ the interface, and $t^n = n\Delta t$ the time mesh. We calculate the mean value of the initial data in each cell as our approximation of the initial data,

$$\rho_j^0 = \frac{1}{\Delta x} \int_{x_{j-\frac{1}{2}}}^{x_{j+\frac{1}{2}}} \rho_0(x)dx.$$

We begin our numerical scheme derivation by assuming that the cell averages at time t^n are known [10], i.e.,

$$\rho_j^n = \frac{1}{\Delta x} \int_{x_{j-\frac{1}{2}}}^{x_{j+\frac{1}{2}}} \rho(t^n, x)dx,$$

and we use a traditional finite volume approach; we begin by defining the piecewise linear interpolants on the cells $[x_{j-\frac{1}{2}}, x_{j+\frac{1}{2}}]$ that approximate the exact solution $\rho(t, x)$ as follows:

$$\tilde{\rho}^n(x) = \rho_j^n + \delta_j^n(x - x_j), \qquad x \in [x_{j-\frac{1}{2}}, x_{j+\frac{1}{2}}], \tag{2}$$

where

$$\delta_j^n \simeq \frac{\partial \rho}{\partial x}\big|_{x=x_i} + o(\Delta x).$$

Taking into account the requirements of conservation, accuracy, and non-oscillation, the evaluation of the gradient δ_j^n is necessarily done by neighboring cells. So, to ensure the non-oscillatory character of the reconstruction and avoid oscillations in the numerical solution, it is necessary to correct it with non-linear operators called limiters. In this work, we choose the generalized limiter of the Van-Leer,

$$\delta_j^n = \frac{1}{\Delta x} minmod \left(\theta \Delta_{j-\frac{1}{2}}^n, \theta \Delta_{j+\frac{1}{2}}^n, \frac{\Delta_{j-\frac{1}{2}}^n + \Delta_{j+\frac{1}{2}}^n}{2} \right), \quad \theta \in [0,1], \quad (3)$$

where $\Delta_{j+\frac{1}{2}}^n$ denote the jump of the solution at the interface $x_{j+\frac{1}{2}}$, i.e, $\Delta_{j+\frac{1}{2}}^n = \rho_{j+1}^n - \rho_j^n$, the minmod function is defined by

$$minmod(a,b) = \begin{cases} sgn(a).\min(|a|,|b|) & \text{if } a.b > 0, \\ 0 & \text{otherwise,} \end{cases}$$

and the value θ will be utilized to regulate the numerical viscosity in the final scheme.

The linear reconstruction $\tilde{\rho}^n(x)$ is evolved to the next time step t^{n+1} by integrating (1) on its staggered cells $[t^n, t^{n+1}] \times [x_j, x_{j+1}]$, providing the following formula:

$$\rho_{j+\frac{1}{2}}^{n+1} = \frac{\rho_j^n + \rho_{j+1}^n}{2} + \frac{\Delta x}{8}(\delta_j^n - \delta_{j+1}^n)$$
$$- \lambda \left(F \left(\rho_{j+1}^{n+\frac{1}{2}}, V_{j+1}^{n+\frac{1}{2}} \right) - F \left(\rho_j^{n+\frac{1}{2}}, V_j^{n+\frac{1}{2}} \right) \right), \quad (4)$$

where $\lambda = \frac{\Delta t}{\Delta x}$ verify the Courant Friedrich Levy (CFL) condition

$$\lambda < \frac{1}{2\lambda_{max}}, \quad \lambda_{max} = \max_{\rho \in [0, \rho_{max}]} \left| \frac{dF(\rho, V)}{d\rho} \right|.$$

In (4), the values at the intermediate time $t^{n+\frac{1}{2}}$ are evaluated by using first-order Taylor expansion and the nonlocal conservation law (1) as follows:

$$\rho_j^{n+\frac{1}{2}} \simeq \rho(t^{n+\frac{1}{2}}, x_j) \quad = \rho(t^n, x_j) + \frac{\Delta t}{2}\rho_t(t^n, x_j) \qquad (5)$$
$$\simeq \rho_j^n - \frac{\Delta t}{2}F_x(\rho(t^n, x_j), V(t^n, x_j)),$$

$$V_j^{n+\frac{1}{2}} \simeq V(t^{n+\frac{1}{2}}, x_j) = V(t^n, x_j) + \frac{\Delta t}{2}V_t(t^n, x_j), \qquad (6)$$

where the space derivative $F_x(\rho(t^n, x_j), V(t^n, x_j))$ in Eq. (6) is approximated by the minmod function

$$F_x(\rho(t^n, x_j), V(t^n, x_j)) = minmod(\theta \left(F(\rho_j^n, V_j^n) - F(\rho_{j-1}^n, V_{j-1}^n) \right),$$
$$\theta \left(F(\rho_{j+1}^n, V_{j+1}^n) - F(\rho_j^n, V_j^n) \right), \frac{F(\rho_{j+1}^n, V_{j+1}^n) - F(\rho_{j-1}^n, V_{j-1}^n)}{2}).$$

We compute the two terms of (6) by the composite trapezoidal rule [2]:

$$V\left(t^{n}, x_{j}\right) = \int_{x_{j}}^{x_{j}+\eta} v\left(\rho\left(t^{n}, y\right)\right) \kappa_{\eta}\left(y - x_{j}\right) dy$$

$$\approx \int_{x_{j}}^{x_{j+\frac{1}{2}}} v(\tilde{\rho}^{n}(y)) \kappa_{\eta}(y - x_{j}) dy$$

$$+ \int_{x_{j+N-\frac{1}{2}}}^{x_{j+N}} v(\tilde{\rho}^{n}(y)) \kappa_{\eta}(y - x_{j}) dy$$

$$+ \sum_{k=1}^{N-1} \int_{x_{j+k-\frac{1}{2}}}^{x_{j+k+\frac{1}{2}}} v(\tilde{\rho}^{n}(y)) \kappa_{\eta}(y - x_{j}) dy$$

$$= \left[\kappa_{\eta}(0) v(\rho_{j}^{n}) + \kappa_{\eta}(\frac{\Delta x}{2}) v(\rho_{j}^{n} + \delta_{j}^{n} \frac{\Delta x}{2}) \right] \frac{\Delta x}{4}$$

$$+ \left[\kappa_{\eta}(x_{N}) v(\rho_{j+N}^{n}) + \kappa_{\eta}(x_{N-\frac{1}{2}}) v\left(\rho_{j+N}^{n} - \delta_{j+N}^{n} \frac{\Delta x}{2} \right) \right] \frac{\Delta x}{4}$$

$$+ \Delta x \sum_{k=1}^{N-1} \kappa_{\eta}(k\Delta x) v(\rho_{j+k}^{n}),$$

and

$$V_{t}\left(t^{n}, x_{j}\right) = \int_{x_{j}}^{x_{j}+\eta} v'\left(\rho\left(t^{n}, y\right)\right) \rho_{t}\left(t^{n}, y\right) \kappa_{\eta}\left(y - x_{j}\right) dy$$

$$= - \int_{x_{j}}^{x_{j}+\eta} v'(\rho(t^{n}, y)) F_{y}\left(\rho(t^{n}, y), V(t^{n}, y)\right) \kappa_{\eta}(y - x_{j}) dy$$

$$= - \left[v'\left(\rho\left(t^{n}, y\right)\right) \kappa_{\eta}\left(y - x_{j}\right) F\left(\rho\left(t^{n}, y\right), V\left(t^{n}, y\right)\right) \right]_{x_{j}}^{x_{j}+\eta}$$

$$+ \int_{x_{j}}^{x_{j}+\eta} \left(v'(\rho(t^{n}, y)) \kappa_{\eta}(y - x_{j}) \right)' F\left(\rho(t^{n}, y), V(t^{n}, y)\right) dy$$

$$= v'\left(\rho_{j}^{n}\right) \kappa_{\eta}\left(0\right) F\left(\rho_{j}^{n}, V_{j}^{n}\right)$$

$$- v'\left(\rho_{j+N}^{n}\right) \kappa_{\eta}\left(x_{N}\right) F\left(\rho_{j+N}^{n}, V_{j+N}^{n}\right)$$

$$+ \frac{\Delta x}{2} \left(v'\left(\rho_{j}^{n}\right) \kappa_{\eta}'\left(0\right) + v''\left(\rho_{j}^{n}\right) \delta_{j}^{n} \kappa_{\eta}\left(0\right) \right) F\left(\rho_{j}^{n}, V_{j}^{n}\right)$$

$$+ \frac{\Delta x}{2} (v' + v)\left(\rho_{j+N}^{n}\right) \left(\kappa_{\eta}' + \delta_{j+N}^{n} \kappa_{\eta}\right)(\eta) F\left(\rho_{j+N}^{n}, V_{j+N}^{n}\right)$$

$$+ \Delta x \sum_{k=1}^{N-1} (v' + v)'(\rho_{j+k}^{n})(\kappa_{\eta}' + \delta_{j+k}^{n} \kappa_{\eta})(x_{k}) F\left(\rho_{j+k}^{n}, V_{j+k}^{n}\right).$$

2.2. **Main result. Unstaggered central schemes.** We begin the construction of our numerical scheme UCS by using Nessyahu-Tadmor's formula (4) to get an estimate $\rho_{j+\frac{1}{2}}$ of the solution at time t^{n+1} on the ghost cells $[x_j; x_{j+1}]$:

$$\rho_{j+\frac{1}{2}}^{n+1} = \frac{\rho_j^n + \rho_{j+1}^n}{2} + \frac{\Delta x}{8}(\delta_j^n - \delta_{j+1}^n)$$
$$- \lambda \left(F\left(\rho_{j+1}^{n+\frac{1}{2}}, V_{j+1}^{n+\frac{1}{2}} \right) - F\left(\rho_j^{n+\frac{1}{2}}, V_j^{n+\frac{1}{2}} \right) \right), \quad (7)$$

and defining the piecewise linear reconstructions of the ghost cell values $\tilde{\rho}_{j+\frac{1}{2}}$:

$$\tilde{\rho}_{j+\frac{1}{2}}(t^{n+1}, x) = \rho_{j+\frac{1}{2}}^{n+1} + \delta_{j+\frac{1}{2}}^{n+1}(x - x_{j+\frac{1}{2}}), \quad x \in [x_j; x_{j+1}], \quad (8)$$

where the slope $\delta_{j+\frac{1}{2}}^{n+1}$ is approximated as in (3) as follows:

$$\delta_{j+\frac{1}{2}}^{n+1} = \frac{1}{\Delta x} minmod \left(\theta \Delta_{j-1}^{n+1}, \theta \Delta_{j+1}^{n+1}, \frac{\Delta_{j-1}^{n+1} + \Delta_{j+1}^{n+1}}{2} \right), \quad (9)$$

where Δ_{j+1}^{n+1} denote the jump of the solution at the cell center x_{j+1}, i.e.,

$$\Delta_{j+1}^n = \rho_{j+\frac{3}{2}}^{n+1} - \rho_{j+\frac{1}{2}}^{n+1}.$$

We then define the solution values ρ_j^{n+1} on the original cell $[x_{j-\frac{1}{2}}; x_{j+\frac{1}{2}}]$ using the formula:

$$\rho_j^{n+1} = (1-\beta)\tilde{\rho}_{j-\frac{1}{2}}\left(t^{n+1}, x_{j-\frac{1}{2}} + \frac{\alpha}{2}\Delta x \right) + \beta\tilde{\rho}_{j+\frac{1}{2}}\left(t^{n+1}, x_{j+\frac{1}{2}} - \frac{\alpha}{2}\Delta x \right), \quad (10)$$

where $(\alpha, \beta) \in [0,1] \times [0,1]$.

Plugging equation (8) into equation (10) leads to:

$$\rho_j^{n+1} = (1-\beta)\rho_{j-\frac{1}{2}}^{n+1} + \beta\rho_{j+\frac{1}{2}}^{n+1} + \left((1-\beta)\delta_{j-\frac{1}{2}}^{n+1} - \beta\delta_{j+\frac{1}{2}}^{n+1} \right)\frac{\alpha\Delta x}{2}. \quad (11)$$

3. Numerical tests

We implement the recommended unstaggered numerical schemes in this part and apply them to traffic flow model problems (1). When we explore numerical tests, the main properties of the proposed schemes will be tested. We will examine the Greenshield velocity function $v(\rho) = v_{\max}\left(1 - \left(\frac{\rho}{\rho_{\max}} \right)^2 \right)$ in all test situations with $v_{\max} = 1$, $\rho_{\max} = 1$, and a limiter parameter value of $\theta = 2$. The CFL condition is set to 0.5, and the look-ahead distance is set at $\eta = 0.1$.

In all tests below, we consider two different initial density distributions: The following smooth initial data is

$$\rho_0(x) = 0.5 + 0.4\sin(\pi x) \quad (12)$$

and the discontinuous one

$$\rho_0(x) = \begin{cases} 0.8 & if \ -1/3 < x < 1/3, \\ 0.2 & \text{otherwise.} \end{cases} \tag{13}$$

For simplicity, we use periodic boundary conditions; we put $f(\rho) = \rho^2/2$ and we restrict the computational domain to $I = [-1, 1]$.

3.1. **Test case 1: Comparison of the schemes.** We start our numerical experiments by comparing the numerical solutions obtained with the UCS scheme and the Nessyahu-Tadmor scheme. First, we set $\Delta x = \frac{2}{400}$ and compute the numerical solution at time $T = 2$; the solution computed is displayed in Figs. 1, 2, and 3. Second, we compare numerical approximations obtained with the UCS scheme for different α's to a reference solution computed with the NT scheme, and $\Delta x = 0.0025$; the solution computed is displayed in Fig. 4. In all figures, the best results are obtained when $\alpha = \frac{1}{2}$.
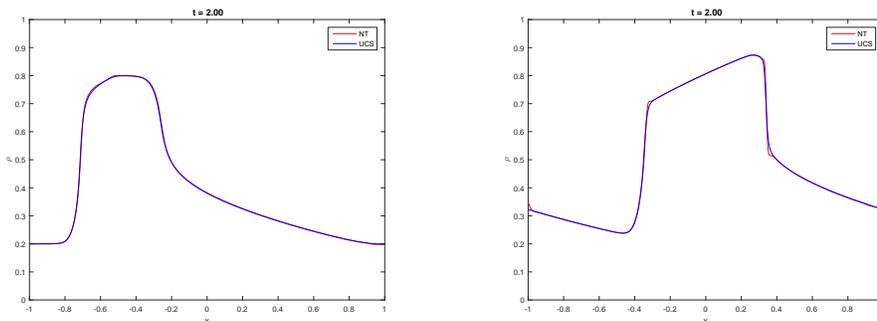
(a) $\alpha = 0.5$

FIGURE 1. Solution of (1), (13) (left); (1), (12) (right). Comparing numerical solution computed with NT and UCS schemes using $\alpha = 0.5$

3.2. **Test case 2: Convergence orders.** We compute the L^1 norm and the order of convergence with respect to mesh size Δx respectively.

$$L^1_{error} = ||\rho_{\Delta x}(T, x) - \rho_{\frac{\Delta x}{2}}(T, x)||_{L^1},$$

$$\gamma(\Delta x) = \log_2 \left(\frac{L^1(\Delta x)}{L^1(\frac{\Delta x}{2})} \right),$$

where $\rho_{\Delta x}$ is the approximate solution computed with a step size Δx. We compare the numerical approximations obtained with $\Delta x = 0.02 \times 2^{-n}$ with $n \in \{0, ..., 4\}$ at time $T = 0.2$ for both schemes. The results of this test are given in Table 1. The L^1 errors of the unstaggered central scheme are nearly
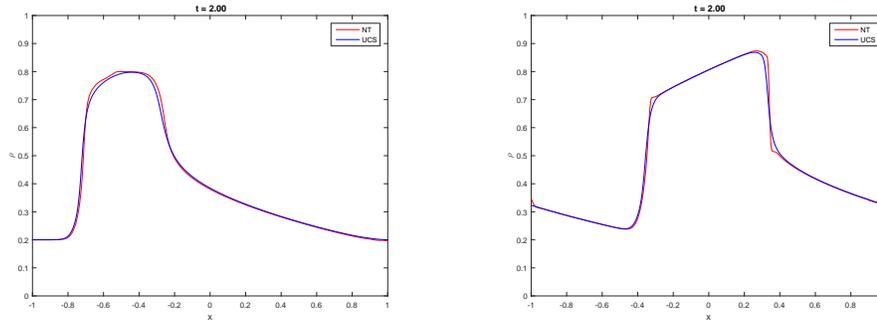
(b) $\alpha = 0.25$

FIGURE 2. Solution of (1), (13) (left); (1), (12) (right). Comparing numerical solutions computed with NT and UCS schemes using $\alpha = 0.25$.
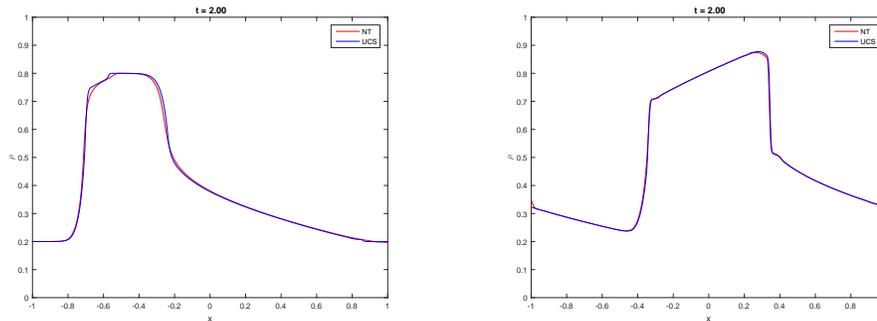

(c) $\alpha = 0.75$

FIGURE 3. Solution of (1), (13) (left); (1), (12) (right). Comparing numerical solutions computed with NT and UCS schemes using $\alpha = 0.75$.

identical to those of the NT scheme. Moreover, the proposed scheme maintains the correct order of convergence.

4. Conclusion

In this study, we have developed unstaggered central schemes for nonlocal traffic flow models. In contrast to the Nessyahu-Tadmor scheme [12], the proposed method evolves the numerical solution on a single grid. Still, it utilizes ghost cells to avoid resolving Riemann problems at cell interfaces. The resulting scheme is easy to implement, second-order accurate, non-oscillatory, and capable of accurately resolving solutions containing discontinuities as well
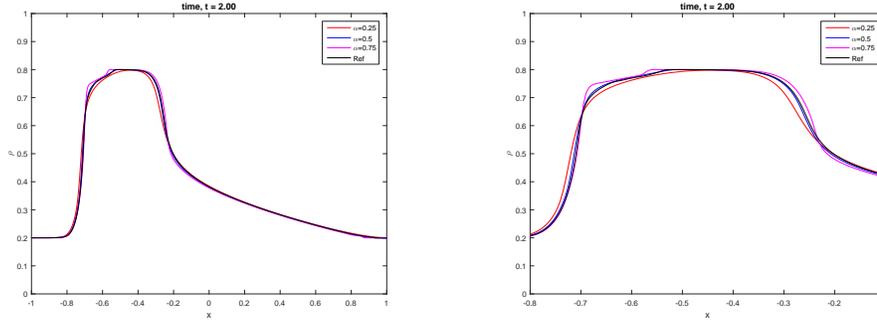
FIGURE 4. Solutions of (1)–(13) computed with UCS for different values of α. Reference solution is computed with NT with $\Delta x = \frac{1}{1600}$ (left); zoom at the shock area (right)
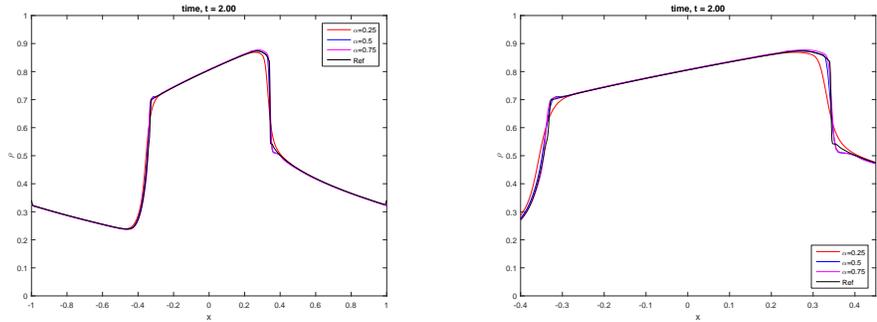

FIGURE 5. Solutions of (1)–(12) computed with UCS for different values of α. Reference solution is computed with NT with $\Delta x = 1/1600$ (left); zoom at the shock area (right)

TABLE 1. Convergence orders and L^1-error at final time $T = 0.2$ corresponding to the initial data (12).

$\frac{1}{\Delta x}$	NT	$\gamma(\Delta x)$	UCS	$\gamma(\Delta x)$
100	8.0253E-05	-	8.0297E-05	-
200	2.0466E-05	1.97	2.0018E-05	2.00
400	5.1592E-06	1.98	5.0059E-06	1.99
800	1.2920E-06	1.99	1.2502E-06	2.00

as achieving their formal convergence rates for sufficiently smooth solutions; it is in good agreement with the corresponding NT scheme, confirming the scheme's ability to handle nonlocal traffic flow models.

References

[1] A. Aggarwal, R.M. Colombo, P. Goatin, Nonlocal systems of conservation laws in several space dimensions, *SIAM J. Numer. Anal.*, **53**, No 2 (2015), 963-983.

[2] S. Belkadi, M. Atounti, Non-oscillatory central scheme for general nonlocal traffic flow models, *Int. J. App. Math.*, **35**, No 4 (2022), 515-528; doi: 10.12732/ijam.v35i4.2.

[3] S. Belkadi, M. Atounti, Central finite volume schemes for nonlocal traffic flow models with arrhenius-type look-ahead rules, *Math. Model. Comput.*, **10**, No 4 (2023), 1100-1108.

[4] F. Betancourt, R. Burger, K.H. Karlsen, E.M. Tory, On nonlocal conservation laws modeling sedimentation. *Nonlinearity*, **24**, No 3 (2011), 855-885.

[5] S. Blandin, P. Goatin, Well-posedness of a conservation law with non-local flux arising in traffic flow modeling, *Numer. Math.*, **132**, No 2 (2016), 217-241.

[6] F.A. Chiarello, P. Goatin, Global entropy weak solutions for general non-local traffic flow models with anisotropic kernel, *ESAIM: M2AN*; doi:10.1051/m2an/2017066.

[7] R.M. Colombo, M. Garavello, M. Lecureux-Mercier, A class of nonlocal models for pedestrian traffic, *Math. Models Methods Appl. Sci.*, **22**, No 4 (2012), 1150023.

[8] J. Friedrich, O. Kolb, S. Gottlich, A Godunov type scheme for a class of LWR traffic flow models with non-local flux, *Netw. Heterog. Media.*, **13**, No 4 (2018), 531–547.

[9] P. Goatin, S. Scialanga, Well-posedness and finite volume approximations of the LWR traffic flow model with non-local velocity, *Netw. Heterog. Media.*, **11**, No 1 (2016), 107–121.

[10] E. Godlewski, P.A. Raviart, *Hyperbolic Systems of Conservation Laws*, Ellipses (1991).

[11] A. Kurganov, A. Polizzi, Non-oscillatory central schemes for a traffic flow model with Arrhenius look-ahead dynamics, *Netw. Heterog. Media.*, **4**, No 3 (2009), 431-451.

[12] H. Nessyahu, E. Tadmor, Non-oscillatory central differencing for hyperbolic conservation laws, *J. Comput. Phys.*, **87** (1990), 408-463.

[13] R. Touma, Central unstaggered finite volume schemes for hyperbolic systems: Applications to unsteady shallow water equations, *Num. App. Math.*, **213**, No 1 (2009), 47–59.

[14] R. Touma, U. Koley, C. Klengenberg, Well-balanced unstaggered central schemes for the Euler equations with gravitation, *SIAM J. Sci. Comput.*, **38**, No 5 (2016), 773–807.